

Seismic waves & climate change



Seismic ocean thermometry

Ocean acoustic tomography: a scheme for large scale monitoring

WALTER MUNK* and CARL WUNSCH†

(Received 4 April 1978; in revised form 3 July 1978; accepted 31 July 1978)

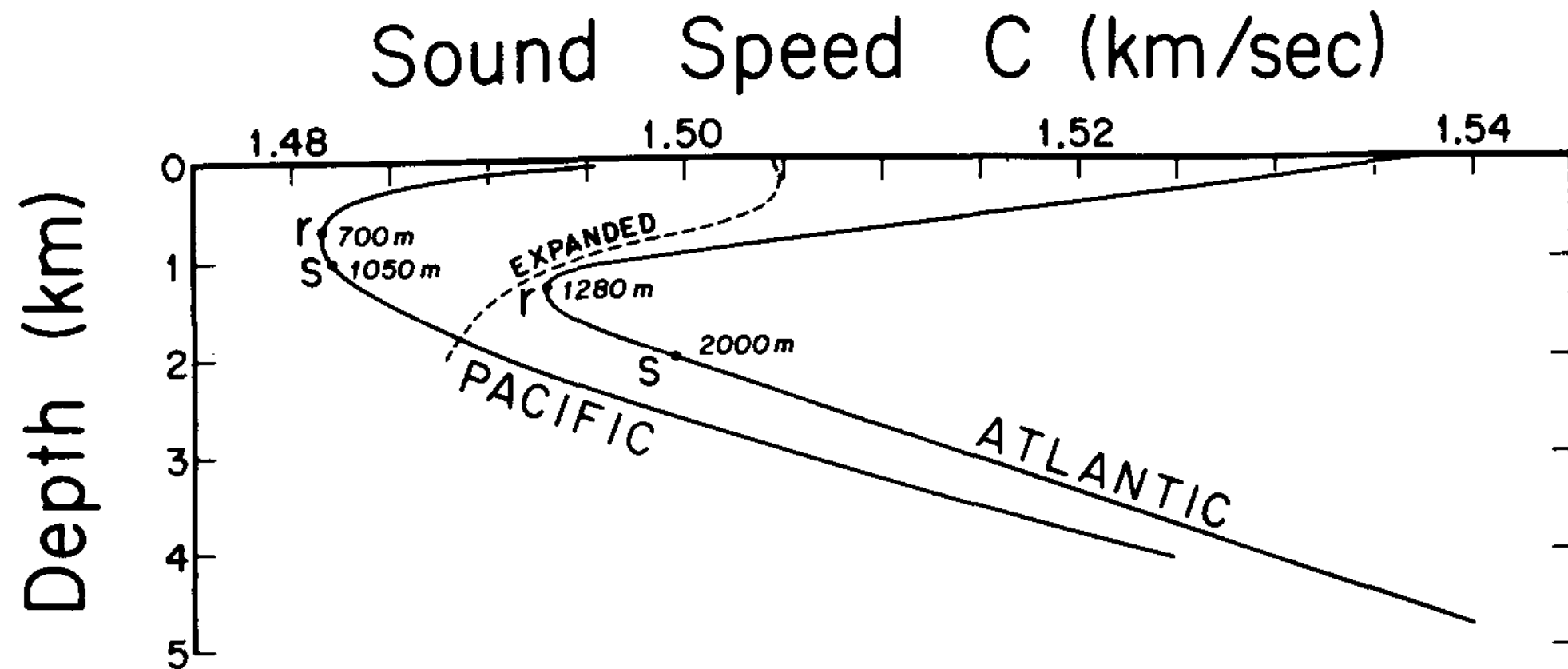
Abstract—We consider the problem of monitoring ocean basins for mesoscale fluctuations, using acoustic inverse techniques. The procedure, which has much in common with conventional seismology, consists of measuring perturbations in travel time between acoustic sources and receivers. Because the number of pieces of information is the *product* of the number of sources, receivers, and resolvable multipath arrivals, the economics of the system is enhanced over usual spot measurements. The temporal resolution required to distinguish multipath arrivals is estimated at 50 ms; the precision required to measure mesoscale perturbations is estimated at 25 ms. The required resolution and precision can be achieved by existing low-frequency (100- to 200-Hz) broadband (> 20 -Hz) sources, but we are ultimately limited to 1000-km ranges by the variable ocean finestructure and associated micropaths. There appear to be no practical range limits imposed by micropaths if such broadband sources could be centered at 30 Hz.

Given the travel time measurements and their noise estimates, we show how actually to invert the system for the interior changes in sound speed and, by inference, for density. The method is analogous to the medical procedure called tomography (from the Greek 'slice'). Measures of the spatial resolution and of formal error bars are obtained. We conclude that such a system is achievable now and has potential for development in a number of directions.

[Munk & Wunsch, 1979]



Seismic ocean thermometry



[Munk & Wunsch, 1979]



Seismic ocean thermometry

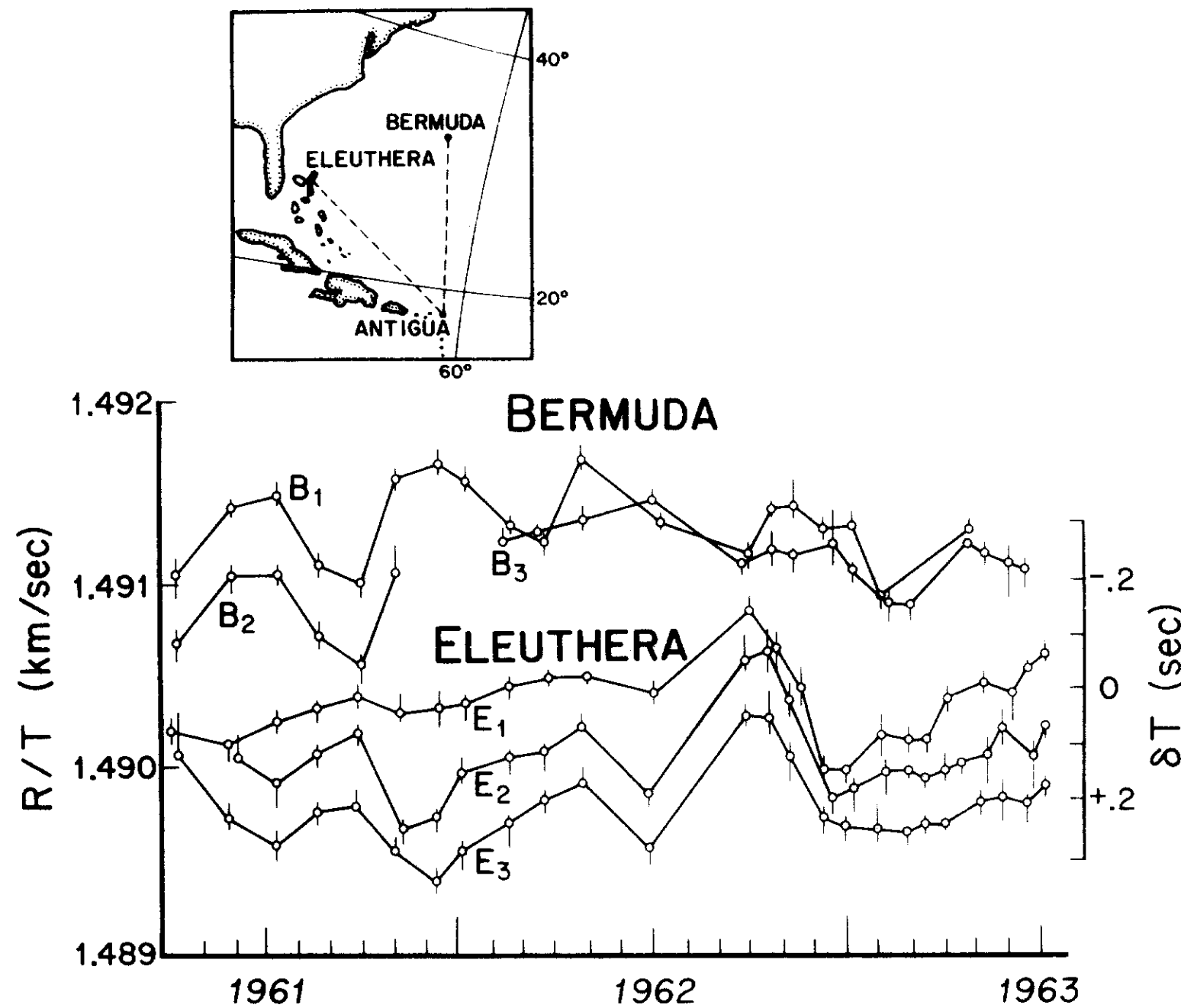


Fig. 3. Variations in the mean axial sound speed R/T and the corresponding perturbation in travel time δT (relative scale), according to HAMILTON (1977). Error bars give full spread of data. The source is at Antigua. Bermuda hydrophone B_1 is tethered 5000 ft above bottom, B_2 is in shallower water on bottom, both are at 875 m beneath the surface. Eleuthera hydrophones E_1 , E_2 , and E_3 are all on bottom at about 1000-m depth.

[Munk & Wunsch, 1979]



Seismic ocean thermometry

OCEAN WARMING

Seismic ocean thermometry

Wenbo Wu^{1*}, Zhongwen Zhan¹, Shirui Peng¹, Sida Ni², Jörn Callies¹

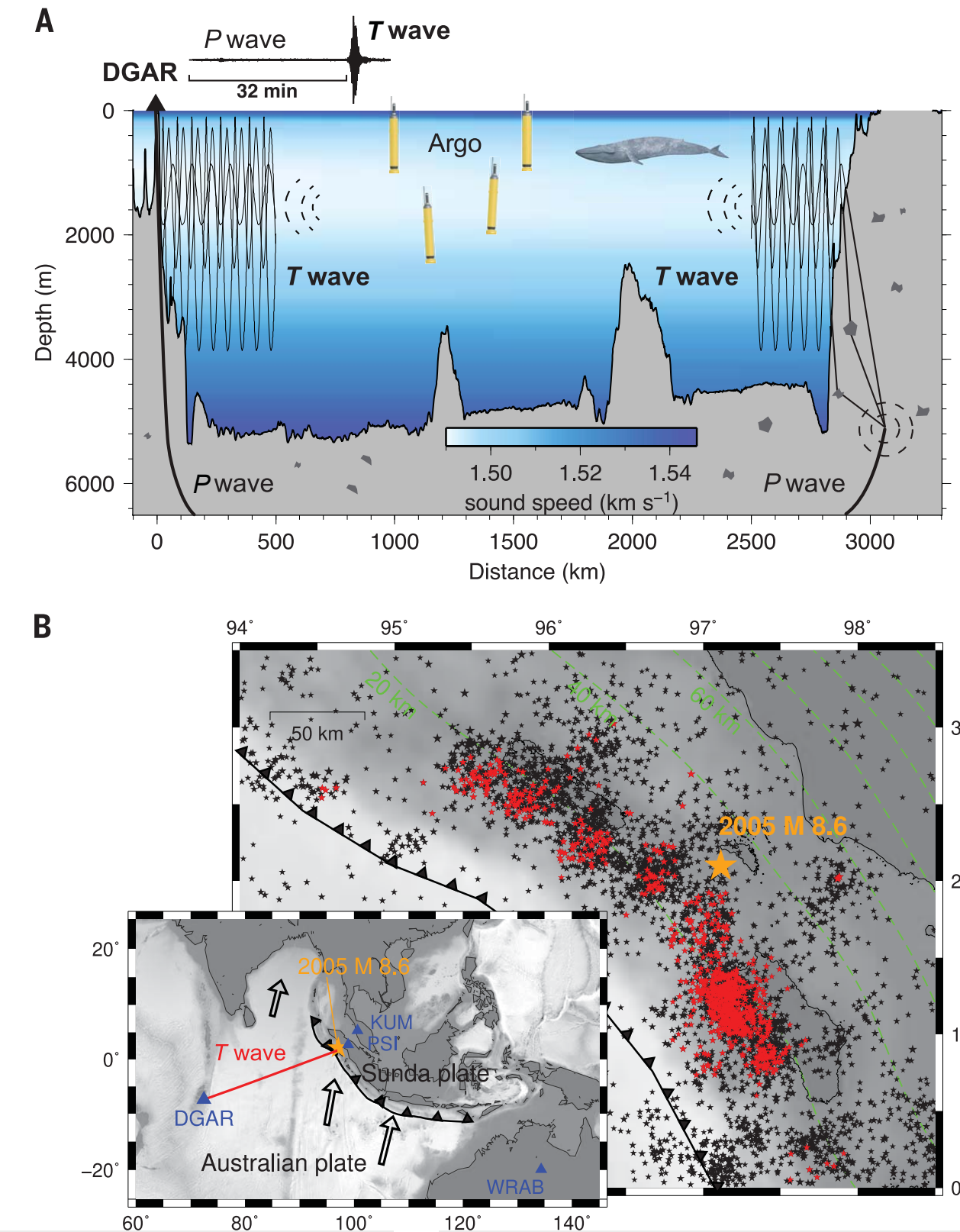
More than 90% of the energy trapped on Earth by increasingly abundant greenhouse gases is absorbed by the ocean. Monitoring the resulting ocean warming remains a challenging sampling problem. To complement existing point measurements, we introduce a method that infers basin-scale deep-ocean temperature changes from the travel times of sound waves that are generated by repeating earthquakes. A first implementation of this seismic ocean thermometry constrains temperature anomalies averaged across a 3000-kilometer-long section in the equatorial East Indian Ocean with a standard error of 0.0060 kelvin. Between 2005 and 2016, we find temperature fluctuations on time scales of 12 months, 6 months, and ~10 days, and we infer a decadal warming trend that substantially exceeds previous estimates.

[Wu et al. 2020]

Seismic waves



Seismic ocean thermometry

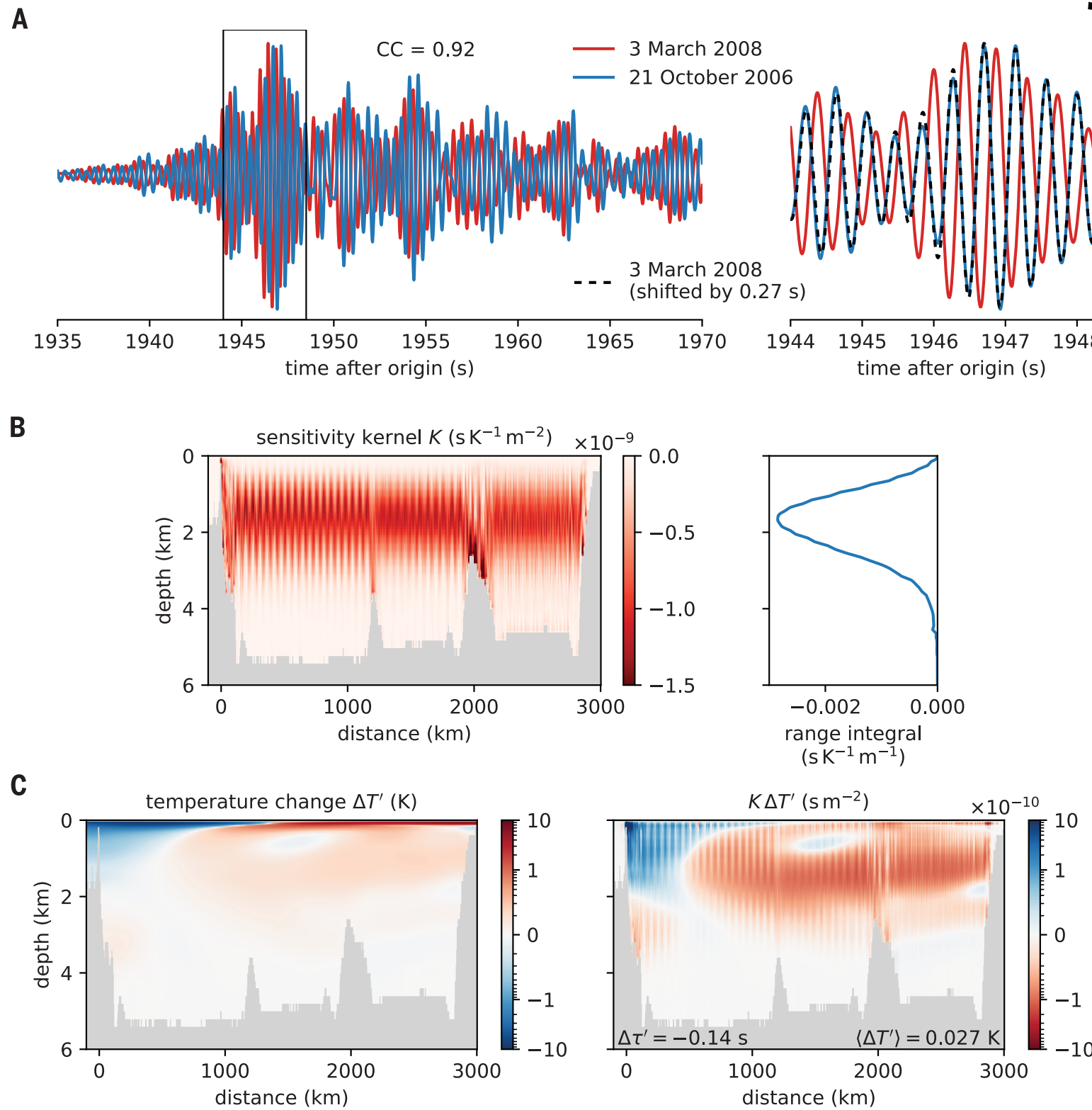


[Wu et al. 2020]

Seismic waves



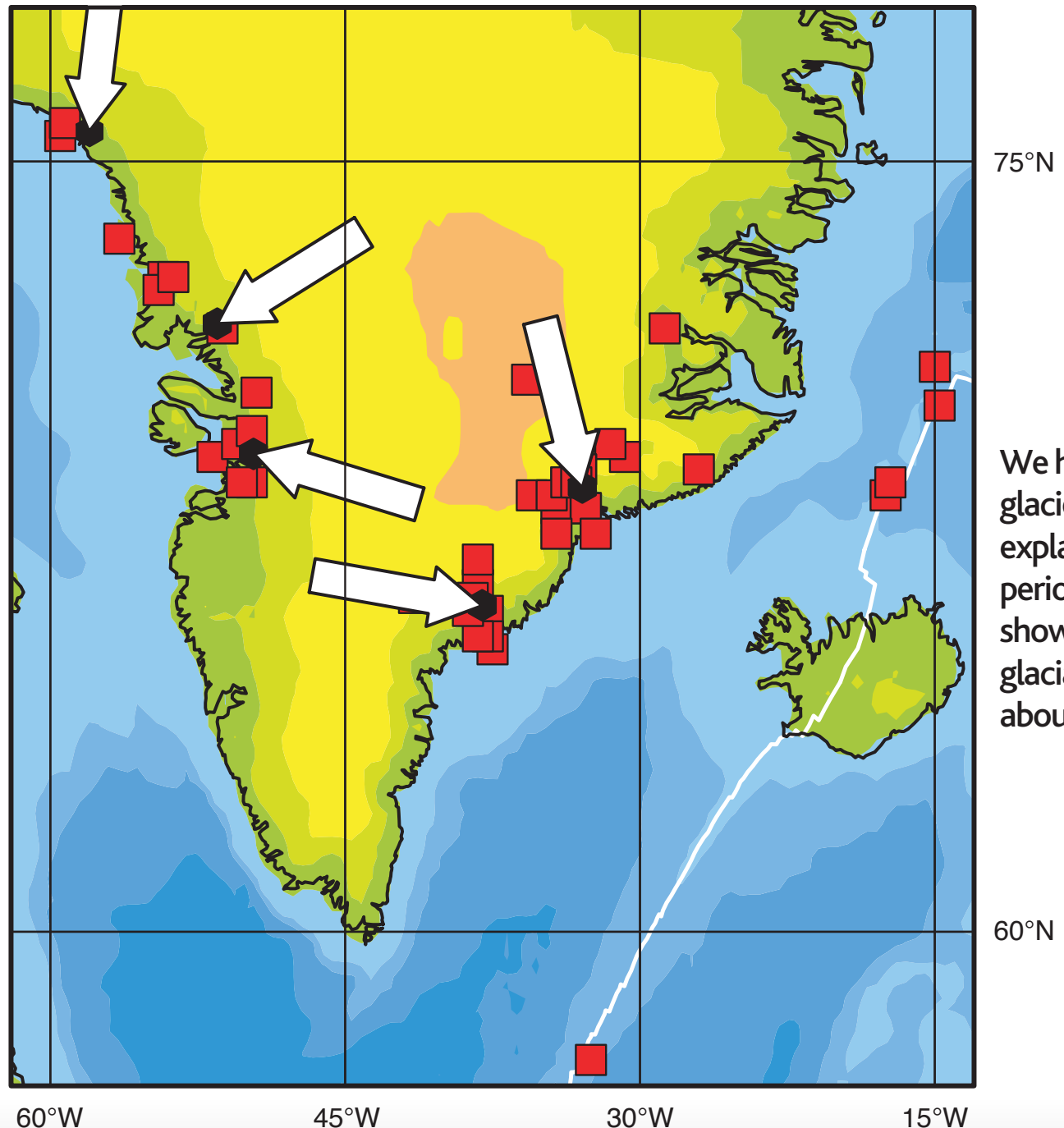
Seismic ocean thermometry



[Wu et al. 2020]



Iceberg calving



Glacial Earthquakes

Göran Ekström,^{1*} Meredith Nettles,¹ Geoffrey A. Abers²

We have detected dozens of previously unknown, moderate earthquakes beneath large glaciers. The seismic radiation from these earthquakes is depleted at high frequencies, explaining their nondetection by traditional methods. Inverse modeling of the long-period seismic waveforms from the best-recorded earthquake, in southern Alaska, shows that the seismic source is well represented by stick-slip, downhill sliding of a glacial ice mass. The duration of sliding in the Alaska earthquake is 30 to 60 seconds, about 15 to 30 times longer than for a regular tectonic earthquake of similar magnitude.

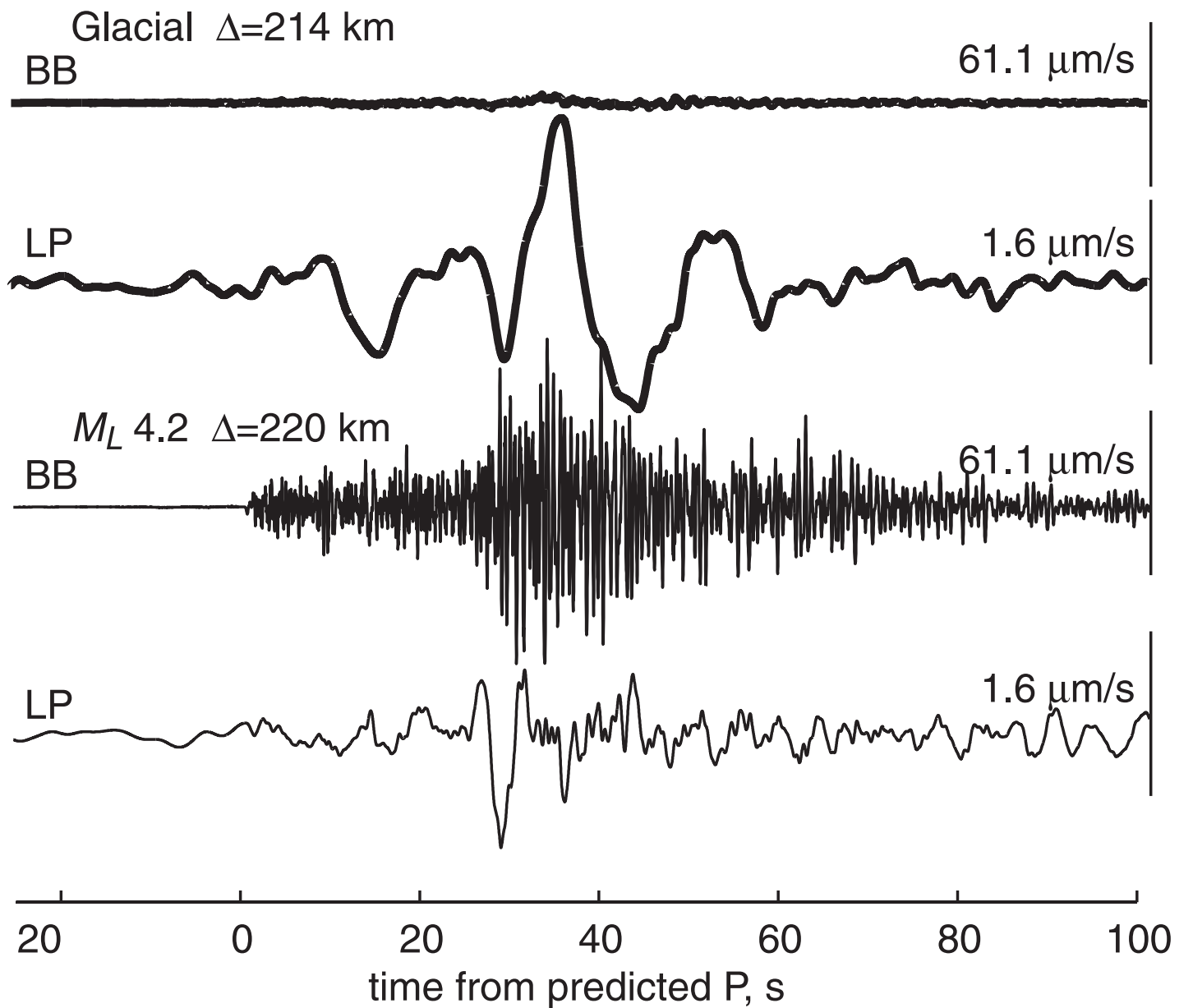
[Ekstrom et al. 2003]

Seismic waves



Iceberg calving

Fig. 3. Seismograms from the Alaska glacial event (4 September 1999, 15:15:20.0) (top two traces) and a nearby, tectonic, $M = 4.2$ earthquake (bottom two traces) recorded at comparable distances (Δ) by BEAAR stations YAN and GOO. For each trace pair, top shows broadband (BB) (0.00833 to 20 Hz) velocity record, and bottom shows filtered long-period (LP) (0.01 to 0.2 Hz) velocity record. Vertical scale is shown by labeled height of line on right. The seismograms are aligned at the predicted P -wave arrival time.



[Ekstrom et al. 2003]



Iceberg calving

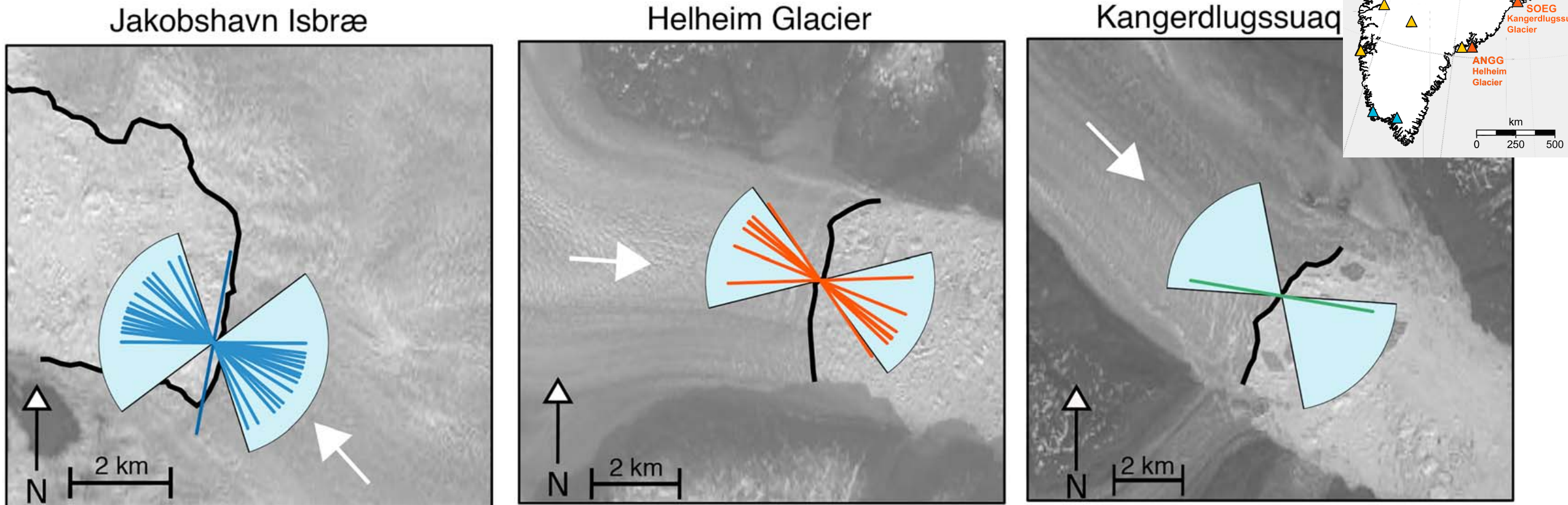


Figure 7. Landsat images from summer 2013 showing each glacier terminus (black line). White arrows indicate direction of glacier flow. Light-blue wedges show the orientation of 95% of published glacial-earthquake force azimuths at each glacier. Colored bars show the orientations of forces we obtain for the small events of this study. The outlying event at Jakobshavn Isbræ corresponds to event 3 in Figure 4 and is discussed in section 5.1.

[Olsen & Nettles 2019]





Glacier Watching Day 17

Seismic waves



chasingice.com



Seismic waves

